

Beam formation

P. Spädtke

GSI, Darmstadt, Germany

Abstract

The quality of a charged particle beam is determined during the generation of the beam. Because the normalized emittance of the beam cannot shrink, beside using special techniques like electron cooling, stochastic cooling, or laser cooling, it is important to avoid errors which are responsible for emittance growth. The specific boundary conditions for the beam formation of different charged particle sources will be described.

1 Introduction

The process of beam formation consists of two different tasks:

- Generation of the required particle species, and,
- to create a beam which has to be transported to the entrance of the accelerator.

Important relations to describe the particle beam or the plasma from which it is extracted with the help of electron density n_e , charge e , electron temperature kT_e , and permittivity ϵ_0 are the Debye length λ_D

$$\lambda_D = \sqrt{\frac{\epsilon_0 k T_e}{e^2 n_e}} \quad (1)$$

or, in practical units:

$$\lambda_D[\text{m}] = 7.43 \cdot \sqrt{\frac{T_e[\text{eV}]}{n_e[\text{cm}^{-3}]}} \quad (2)$$

and the plasma frequency ω_p with the electron mass m_e :

$$\omega_p = \frac{e^2 n_e}{\epsilon_0 m_e} \quad (3)$$

or, in practical units for electrons:

$$\omega_{pe}[\text{Hz}] = 8980 \cdot n_e[\text{cm}^{-3}] \quad (4)$$

and for ions with mass A and ion density n_i :

$$\omega_{pi}[\text{Hz}] = 210 \cdot q \cdot \frac{n_i[\text{cm}^{-3}]}{A[\text{amu}]} \quad (5)$$

To compare different particle sources with each other the perveance has been defined as:

$$P = I/\Phi^{1.5} \quad (6)$$

As a quality measure the beam emittance is used for accelerator applications. In general the beam emittance describes the distribution of particles in the 6-dimensional phase space x, y, z, v_x, v_y, v_z at a given time t .

Under certain conditions this phase space can be restricted to lower rank subspaces. In accelerator physics the longitudinal 2-dimensional phase space can be assumed to be independent from the 4-dimensional transverse phase space. The other two components of the momentum can be described as small angles between the transverse and the longitudinal momentum component.

$$x' = v_x/v_z \quad (7)$$

$$y' = v_y/v_z . \quad (8)$$

If there is no dependency or coupling between both these transverse phase spaces they can be subdivided in two 2-dimensional phase spaces. This is valid for example for an electron gun with a diode extraction system without magnetic fields. However, it becomes different if magnetic fields are present, coupling both transverse phase spaces with each other. Any velocity component perpendicular to the magnetic field vector \vec{B} will cause a force \vec{F} coupling both transverse phase spaces.

$$\vec{F} = q(\vec{E} + \vec{v} \times \vec{B}) . \quad (9)$$

It should be pointed out, that even for a ‘zero’ temperature beam there is a reason for a transverse force caused by the internal space charge. With the assumption of a cylindrical beam within a grounded beam tube with radius r_w and with a homogeneous density distribution this space charge creates a potential which is parabolic inside the beam and logarithmic outside the beam:

$$\Phi = \frac{I}{4\pi\epsilon_0\beta c} \left(1 + 2 \cdot \ln \frac{r_w}{r} - \frac{r^2}{r_b^2}\right) \quad \text{inside the beam} \quad (10)$$

$$\Phi = \frac{I}{2\pi\epsilon_0\beta c} \ln \frac{r_w}{r} \quad \text{outside the beam} . \quad (11)$$

This potential causes that charged particles closer to the axis become more decelerated than charged particles closer to the beam edge. Due to the coupling the beam has to be described in the 4-dimensional phase space.

There are other reasons for radial electric fields, generating a radial force on the beam, as for example any aperture in an electrode with a different potential than the surrounding.

2 Electron beam generation

Electrons can be generated by transfer of sufficient energy to the electrons so that they are able to escape from a cathode into vacuum. Transfer of energy might be performed by heating the cathode, by exposing the cathode to photons, applying a high electric field in front of the cathode, or comparable methods.

As soon as the electrons have left the cathode material, they participate in the process of beam generation. Depending on the total number of electrons with relation to the extraction field strength the state of beam generation is either called emission limited flow, respectively space charge limited flow. As long as the gradient $d\Phi/dz$ in front of the cathode is positive the process is called emission limited, when the gradient becomes zero the space charge limited emission has been reached. Note, that if a negative gradient would be present, electrons leaving the cathode would be decelerated and reflected towards the cathode again.

This behaviour is described by the law of Child–Langmuir [3,4]:

$$j = \frac{4}{9}\epsilon_0 \sqrt{\frac{2q}{m_i}} \Phi^{1.5}/d^2 . \quad (12)$$

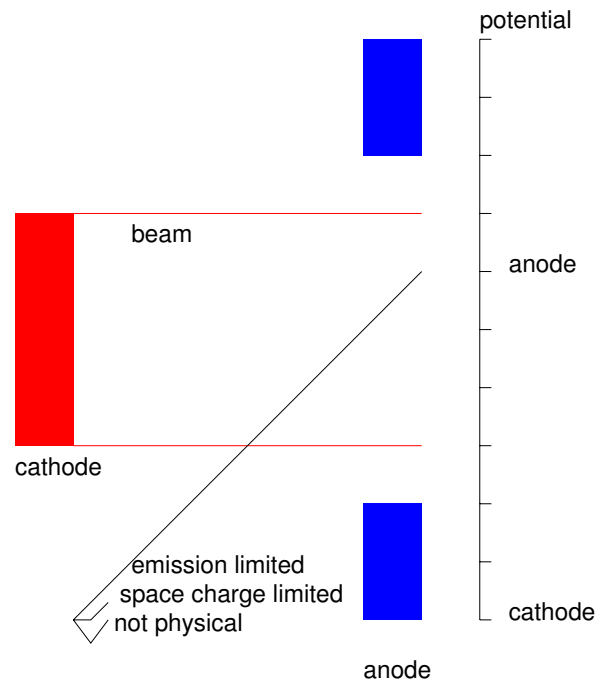


Fig. 1: Potential on mid axis in front of the cathode for the three different current densities

The space charge limited current density j depends on the potential drop Φ across the extraction gap width d . For ions j depends on the mass m_i and charge q . As a consequence, to create a beam of fixed current and variable energy either the emission capability has to be influenced, or a three electrode system, a triode instead of a diode has to be used.

If desired, it can be tried to compensate transverse velocity components, for example by two electrodes with suitable spacing, cancelling the effect of each other. This is called resonant focusing. Further reading: Ref. [1]. Such an optimization is necessary for electron guns for electrode cooling, where an electron beam with lowest possible transverse energy is required to provide optimum cooling conditions for the stored ions. As an example, the electron cooler device in the ESR at GSI is shown in Fig. 4. Further reading: <http://www.gsi.de>.

Because of the large range of ion beam energy the required electron beam energy is up to 300 keV. The required voltage is separated into a cathode-anode voltage drop, defining the electron beam current of up to 5 A, and an additional voltage drop to accelerate the electron beam to the velocity of the stored ion beam, see Fig. 3. The beam is embedded in a magnetic field of 0.2 T from the cathode to the collector. The magnetic field is made by the gun solenoid, a toroidal section with two magnetic toroids, the cooler solenoid, again a toroidal section, and the collector solenoid, see Fig. 4. This collector solenoid is made by two different coils to increase the electron beam diameter to keep the local power density as small as possible. To decrease the power which is dissipated in the vacuum furthermore, the beam is decelerated again before entering the collector, decreasing the loss power from 1.5 MW to 25 kW.

3 Ion beam generation

Depending on the required particle, different physical processes might be available to generate their ionic state. These processes will be described for the mentioned ion sources. Not to extend the list of references they are not included here, but can be found in the suggested further readings. A summary of latest developments can be found in the conference proceedings of the International Conference on Ion Sources (ICIS) published by RSI, which takes place every two years.

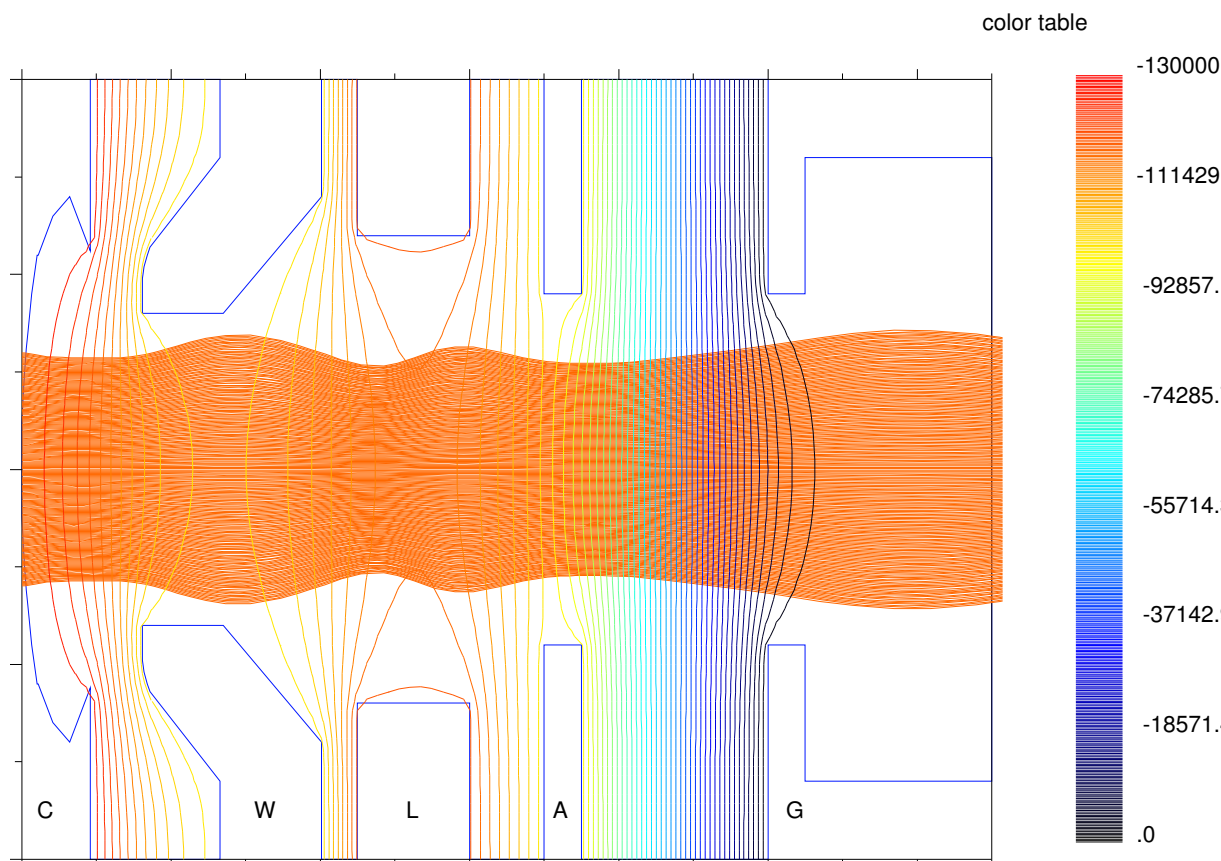


Fig. 2: Electron gun with cathode (C), a Wehnelt electrode (W) to control the current, an Einzel lens (L) to match the beam to the acceleration gap between anode (A) and ground (G). Potential lines are displayed together with electron trajectories.

3.1 General

Beam generation for ions is somewhat more complicated, compared to electrons. This is not only because of ions from different elements have to be provided from ^1H to ^{238}U , but also different charge states, see Fig. 5 for the wide range of necessary electron energies, different isotopes, sometimes even compounds of different elements, up to giant molecules. Therefore, it is not surprising, that there are a lot of different ion sources: discharge ion sources like Freeman type, PIG, magnetic cusp ion sources, cathode free ion sources such as rf-sources, electron cyclotron resonance ion sources (ECR), laser ion sources (LIS), electron beam ion sources (EBIS), vacuum arc ion sources, surface ionization ion sources, and negative ion sources is a list of totally different devices, far away from being complete. All of these different generation processes do have advantages and disadvantages with respect to any specific application; no general classification which source is the best is available.

In general, all plasma sources will generate a plasma from the neutral gas provided to the discharge. If ions are required from non-volatile elements, additional effort is necessary to provide these atoms to the discharge. Common techniques are evaporation, sputtering, chemical compounds, chemical reaction, erosion by discharge, or erosion by ablation.

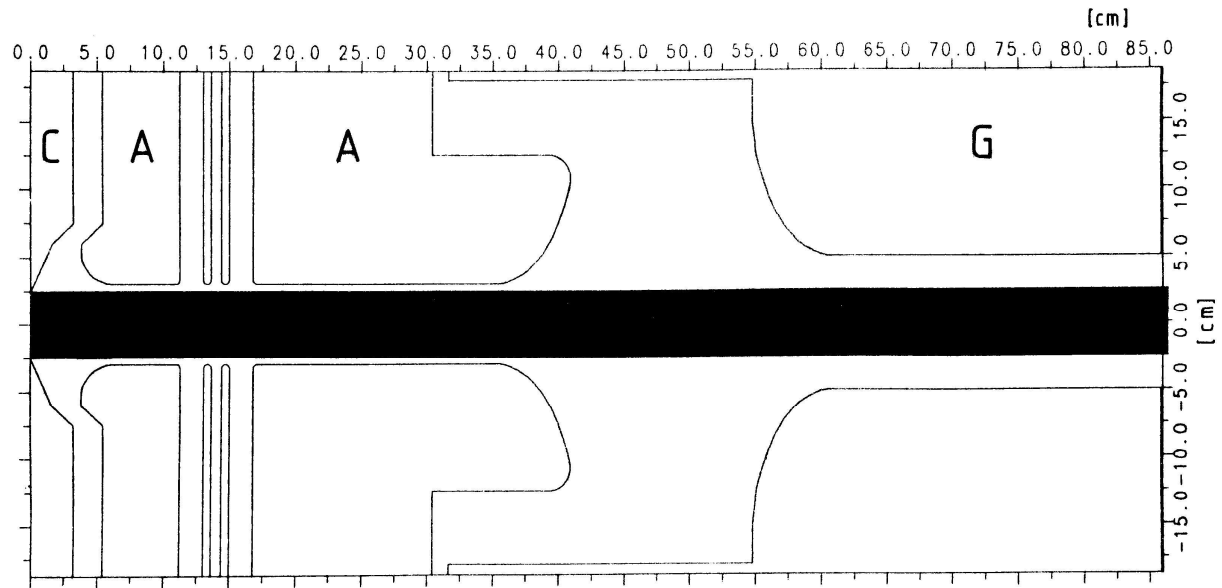


Fig. 3: Electron gun with cathode (C), anode (A), and ground electrode (G). The anode is split in two different electrodes with two additional electrodes for optional resonant focusing.

3.2 Specific ion sources

3.2.1 Cusp sources

A directly heated or indirectly heated cathode provides electrons for the discharge, which is typically a low voltage discharge. To increase the number of electrons together with the efficiency of the discharge, the loss area for electrons is minimized by a magnetic field. In most cases a solenoidal field in longitudinal direction or a transverse cusp field is used. Combinations of both field forms are possible. However, to avoid plasma instabilities, the loss area has to be large enough to avoid instabilities.

Electrons from the cathode will be accelerated into the plasma and might collide with a neutral atom, resulting in an ionization and producing a positive ion and an electron. The resulting plasma is typically cold, temperatures in the lower eV range are possible. This advantage has to be paid by the fact that mainly singly charged ions will be produced. Inside the source chamber this plasma is contained at plasma potential, which is typically a few volt below anode potential, see Fig. 6, showing the CHORDIS cusp source.

A larger discharge volume and a better magnetic confinement, due to the better positioning of the magnets result in a charge state distribution shifted towards higher charge states for another type of cusp source, called MUCIS, see Fig. 7. Whereas for the CHORDIS the maximum intensity for argon operation is found in Ar^{1+} , the MUCIS has its maximum in Ar^{2+} . Close to the extraction hole ions will be accelerated, electrons will be decelerated and reflected into the plasma, leaving the ions alone with their space charge. This interface between plasma and extracted beam is called plasma boundary. Depending on the electron temperature this sheath is a few volts thick, see Eqs. (1),(2). The location depends on the external gradient $d\Phi/dz$ and the plasma pressure. This behaviour is demonstrated in a computer simulation, see Fig. 20, where the plasma pressure has been changed from 50 mA/cm^2 to 300 mA/cm^2 .

After extraction the beam will drift with the velocity gained by $v_0 + \sqrt{\frac{2qU}{m}}$. v_0 can be neglected in most cases, because of the low energy of the ions inside the plasma. However, there is an internal, repulsive force: the space charge.

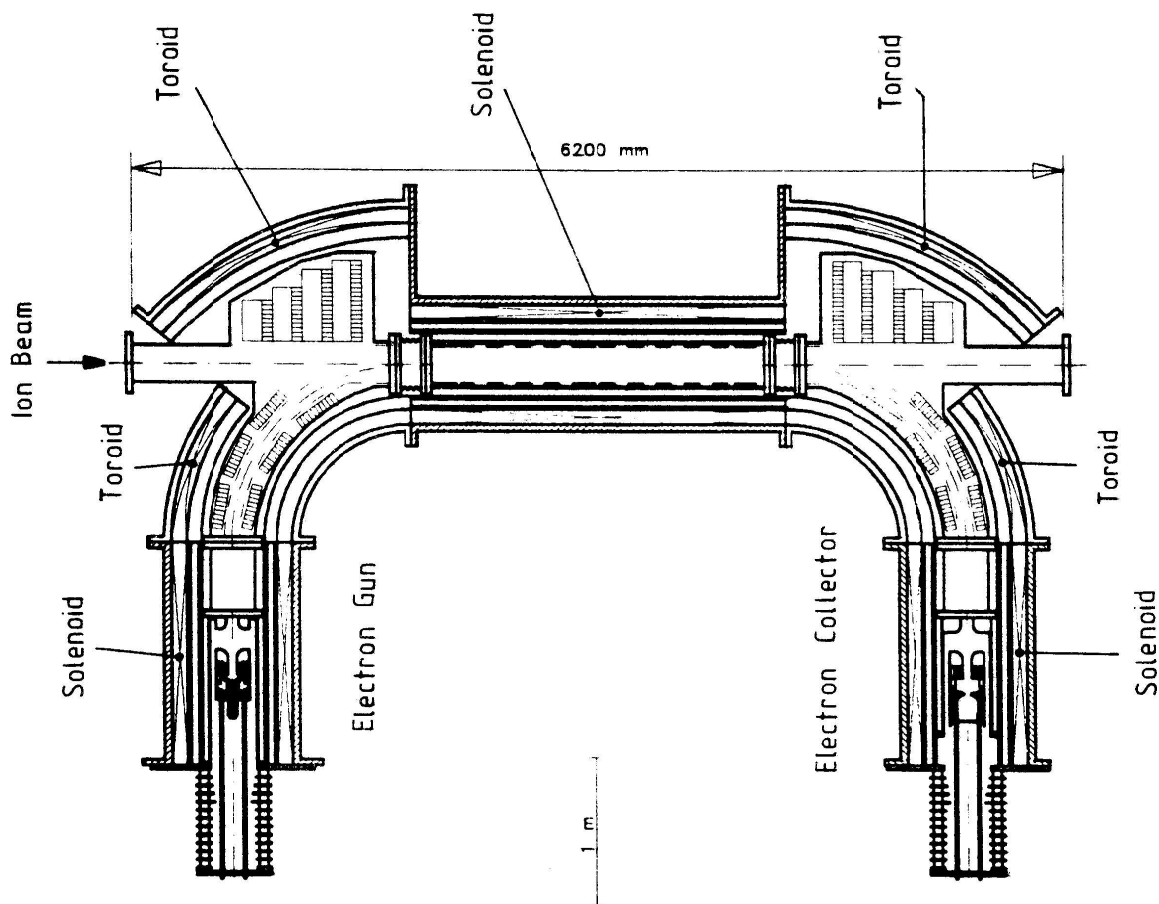


Fig. 4: Electron cooler

3.2.2 ECRIS

This type of ion source does not have a filament. There is no cathode and no anode. The element to be ionized is fed into the source in gaseous form. Guiding rf-power with frequencies above 1 GHz into the source can transfer energy to electrons which ionize the gas atoms. To keep the electrons within the source chamber a magnetic field is applied. This magnetic field has a special shape. A solenoidal field is superimposed by a radial field. In most cases a hexapolar field is used for the radial component, quadrupole fields, decapole fields, and octupole fields have also been tried. To keep the electrons within the discharge chamber a certain resonance condition between the resonance frequency of the applied rf and the applied magnetic field has to be fulfilled:

$$f[\text{GHz}] = 28 \cdot |B[\text{T}]|. \quad (13)$$

With such a configuration the plasma is confined in a so-called minimum B structure, see Fig. 9. By step-wise ionization the mean charge state can be increased considerably. Several measures were applied to ECR sources to increase their performance furthermore:

- mixing gas cooling effect, atomic physics.
- biased probe influencing secondary electron emission, plasma physics.
- specific chamber materials influencing the secondary electron generation.

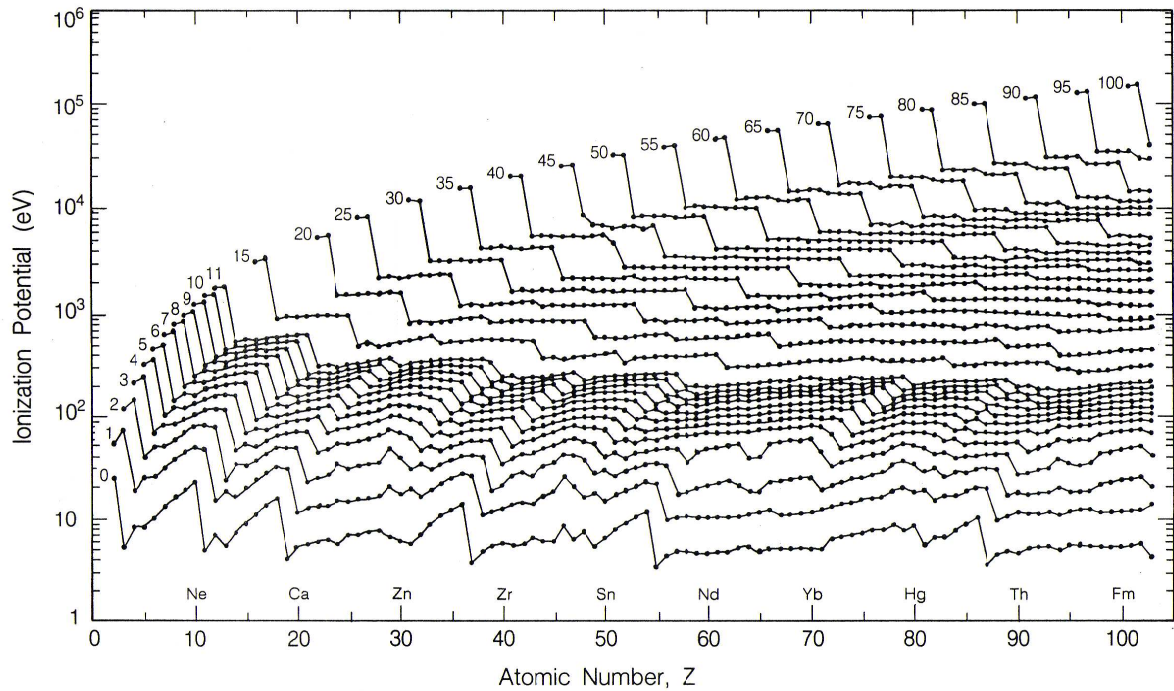


Fig. 5: Ionization energies for different elements and different charge states

– afterglow/puma

influencing the confined plasma.

Even though the plasma generator is highly advanced, the beam extraction is more difficult compared to other sources. This is due to the specific magnetic field structure and the composition of the extracted beam, which is a mixture of different charge states. In most cases the plasma density is not homogeneous across the extraction aperture, resulting in undesired nonlinear electric forces, rearranging the ion distribution to make it homogeneous again. This will happen at the expense of an increase of emittance.

Particularities obtained in the extraction system for an ECR ion source:

- the lower the radial electric fields close to the plasma boundary are, the lower the radial velocities of the ions, therefore low force due to $\vec{v} \times \vec{B}$. Note that the direction of the magnetic field is in longitudinal direction. This minimizes the azimuthal velocity component, reducing a radial force on the ions. Therefore a flat plasma boundary seems to be best. In that case the plasma pressure cancels the radial component of the electrostatic field caused by the applied extraction voltage.
- This requires on the other hand that the plasma pressure is constant in azimuthal direction, a contradiction because of the hexapolar field present in ECRIS and the condition of a minimum B structure.

3.2.3 Afterglow

An ECRIS can be operated in a pulsed mode, which provides the possibility to trap highly charged ions in the plasma. By switching off the rf-power this trap is opened and releases all ions within a time of up

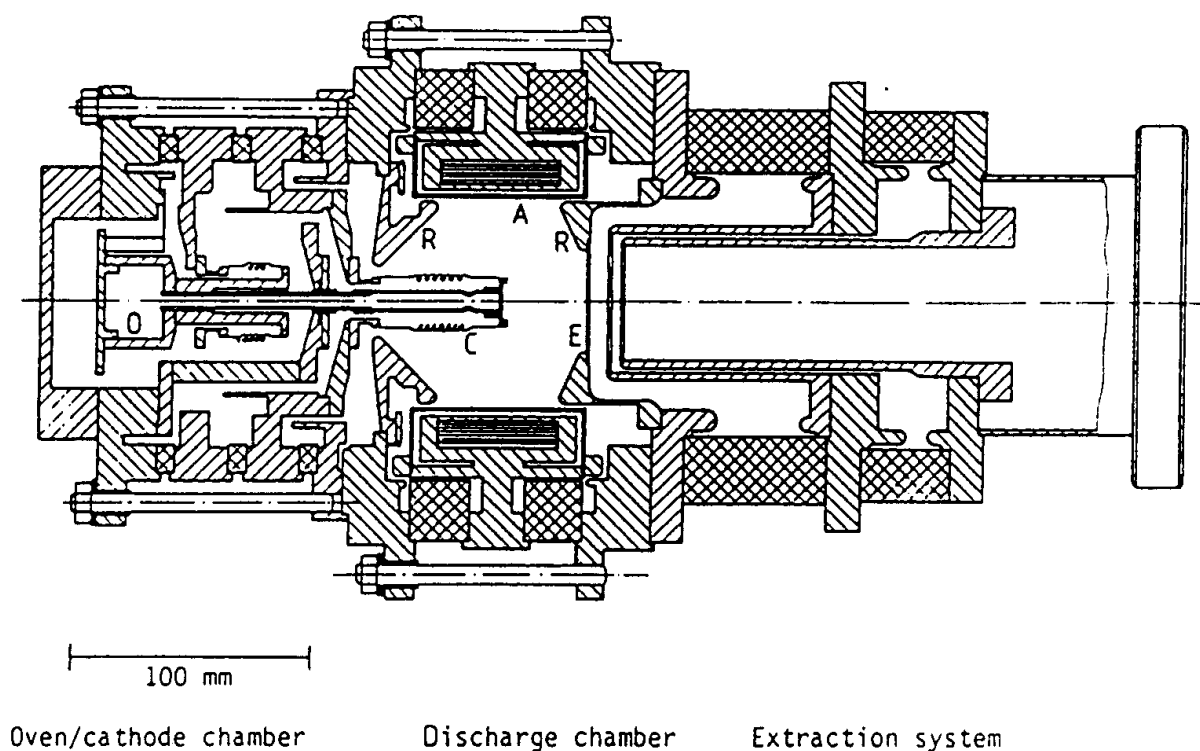


Fig. 6: CHORDIS multi cusp ion source. Permanent magnets placed directly behind the anode (A) create a cusp field in radial direction. The cathode (C) is a hot filament cathode, reflector electrodes (R) confine the plasma electrostatically. The oven (O) is used for non volatile elements. Extraction electrodes (E) are on the right.

to milliseconds, see Fig. 10.

3.2.4 PUMA

A similar effect can be invoked by a different physical method, namely to pulse the magnetic field to push all ions towards extraction. The extraction from this source has to take this additional momentum into account as well as the increased space charge force due to the high ion density.

Further reading: D. Leitner and C. Lyneis in Refs. [8], [10], [12].

3.2.5 Freeman source, PIG

Electrons are provided to the discharge by a heated cathode. These electrons are accelerated towards the anode. A magnetic field increases the impedance for these electrons.

Because of the higher voltage between cathode and anode, compared to cusp sources, the electron energy is higher, therefore higher charge states are expected. This can be further optimized using a cold cathode. To create metallic ions a sputter electrode is used at GSI. A part of the discharge current is drawn to a sputter electrode, which is biased negatively with respect to the plasma. Only neutrals coming from the surface of the sputter electrode are able to drift into the plasma, where they can be ionized and extracted.

BEAM FORMATION

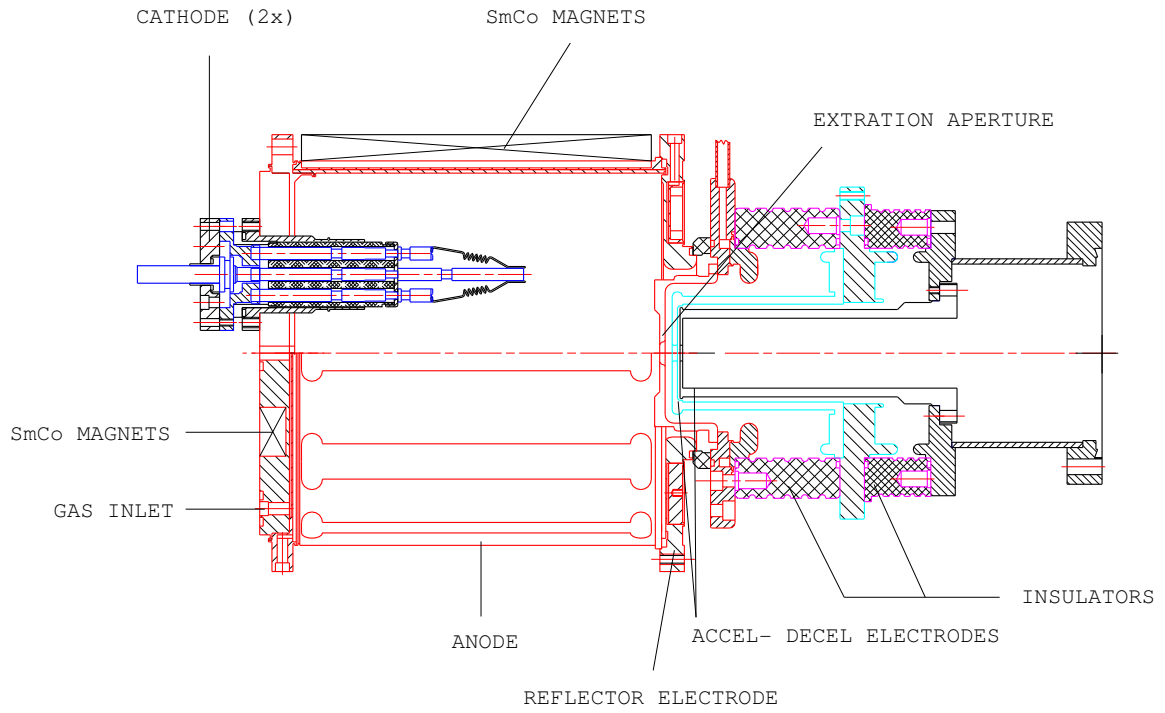


Fig. 7: MUCIS multi cusp ion source

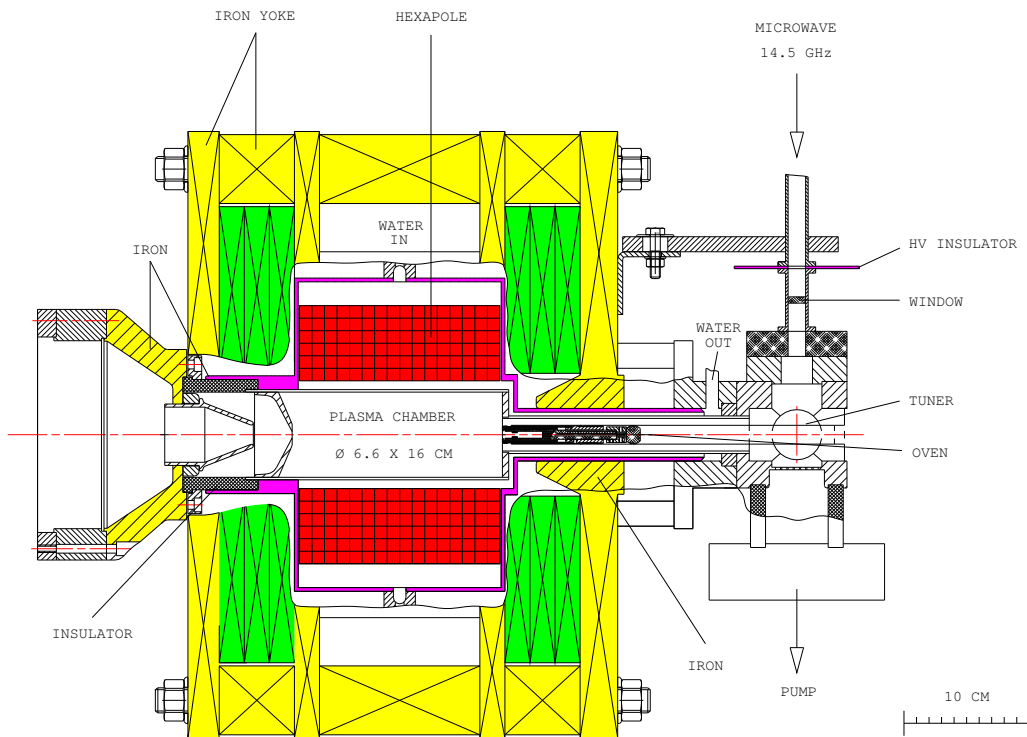


Fig. 8: CAPRICE ion source

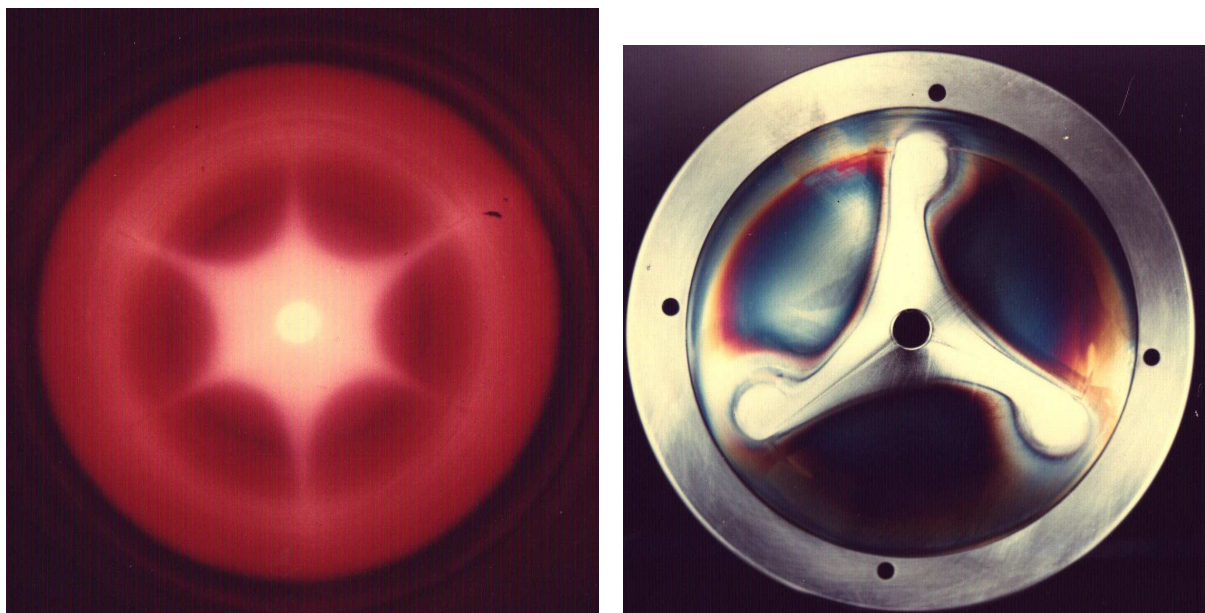


Fig. 9: Radial shape of the plasma inside the plasma chamber (left) and sputter marks of the plasma on the plasma electrode (right)

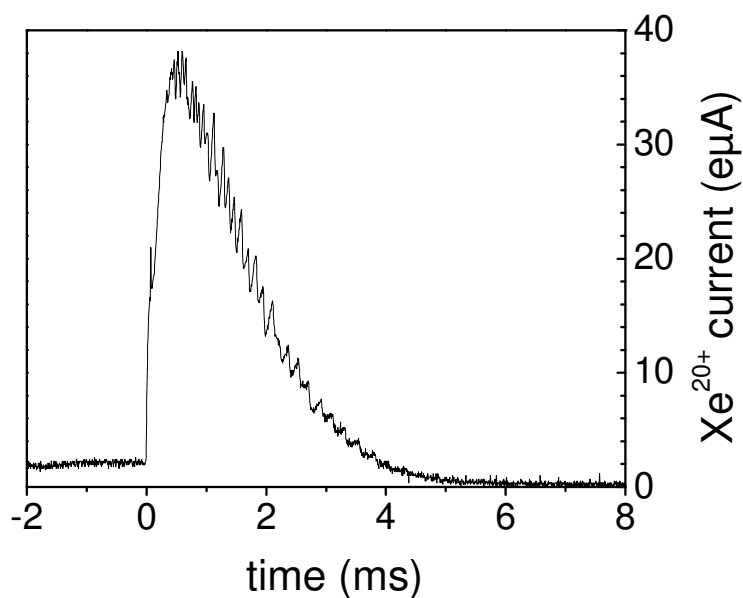


Fig. 10: Analysed current signal for the afterglow of Xe^{20+} . The rf power is switched off at time 0, releasing the trapped ions.

3.2.6 Radial extraction

The magnetic field is perpendicular to beam extraction, which implies several consequences:

- Owing to the shape of the plasma, a slit extraction is suitable.
- Different charge states which are inside the plasma will be extracted on different trajectories, see Fig. 13.
- Cold electrons inside the plasma are fixed to the magnetic field lines, determining the plasma

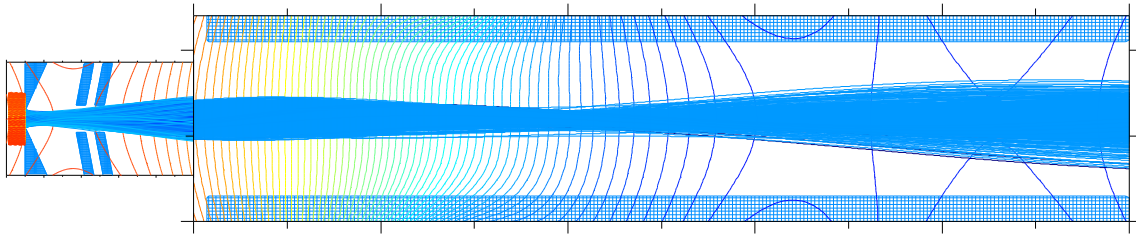


Fig. 11: Geometry and lines of constant magnetic flux density in beam direction. The location of the maximum flux density is close to the negative screening electrode. Within the region of extraction the flux density drops from 3.3 T to 3.0 T, in the beam line a solenoidal lens focuses the beam.

boundary.

- Electrons in the extracted beam cannot penetrate the extraction system due to the magnetic field, therefore a triode extraction system working in accel-decel mode is not necessary.
- The alignment of the extraction electrodes should take the magnetic field into account.

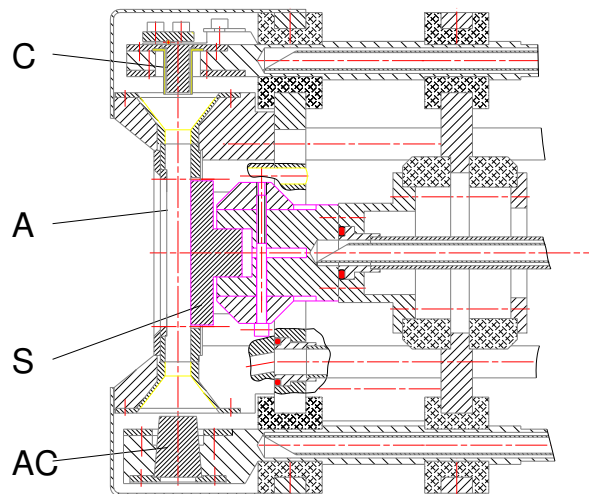


Fig. 12: Side view of a Penning ion source with heated cathode (C), cold anticathode (AC), anode (A), and sputter electrode (S). The magnetic field points in the direction from cathode to anticathode.

3.2.7 Axial extraction

In this case the ions are extracted through a hole in the cathode. This situation is similar to the extraction from an ECRIS, beside the missing hexapole.

Further reading: D. Aitken in [7], and M. Farley, P. Rose, and G. Ryding in [8].

3.2.8 Vacuum arc ion sources

If ion beams of metals are required, this type of ion source should be taken into consideration. A voltage is applied between a cold cathode, made out of the required material, and an anode. The discharge in the order of up to several 100 A is ignited by a trigger. The trigger is usually a high voltage spark, but other methods can be used as well. The discharge is supported by a number of smaller current arcs of about

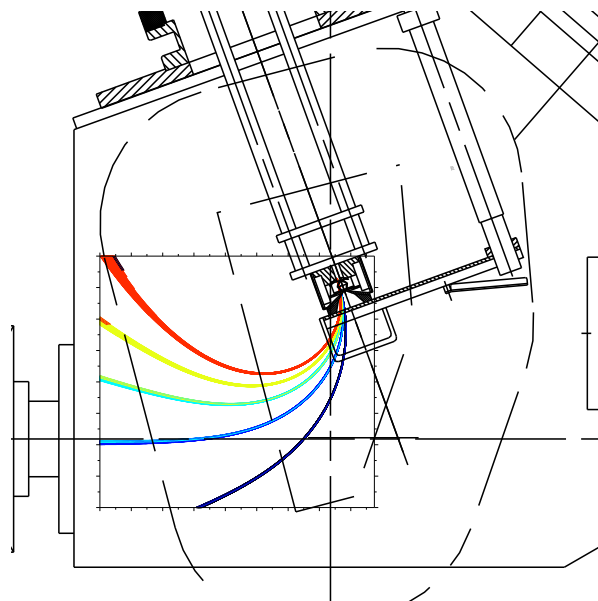


Fig. 13: Top view of a PIG source with an extraction system inside a 110° source dipole magnet, and the vacuum beam line. The rectangular insertion shows the region of computation together with an extracted Argon beam with charge states 1 to 5. Charge state 2 has been selected for the accelerator. A fully space charge compensated beam is assumed.

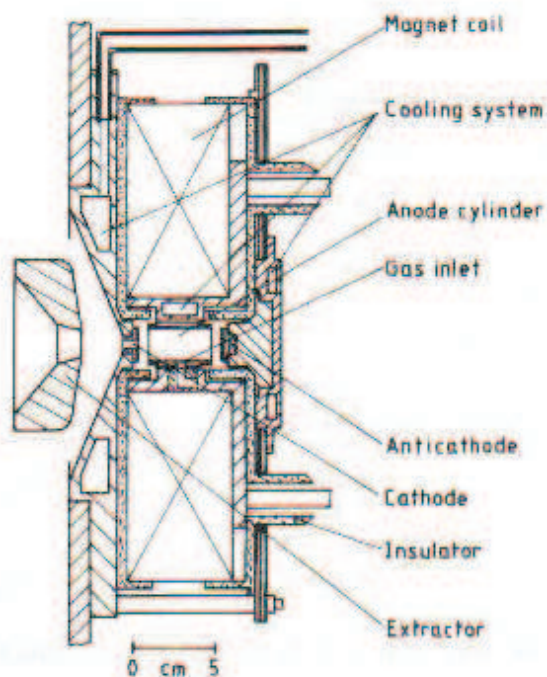


Fig. 14: Penning ion source, axial extraction

5 A each with a lifetime in the order of microseconds which is the reason for the statistical behaviour of this type of discharge (analysing the noise signal has not shown any preferred frequencies). The cathode material is explosively evaporated by the discharge. Because of the very high local discharge power the

cathode material is not only evaporated, but also ionized. The charge state distribution is frozen after a short distance behind the cathode.

The generated plasma drifts through a hole in the anode towards the extraction electrode. Up to several ampere of ion current have been extracted from such a plasma. Because the acceptance of an accelerator is typically small and the brightness of the extracted ion beam is a limited quantity, these currents are not available at an accelerator. But the achievable plasma density is at least high enough to match the current density given by Child's law.

Because of the statistical behaviour of the discharge process a noisy plasma (spatial density fluctuation with time), resulting in a noisy extracted beam as well. Whereas this effect is not important for applications with time integrated dose requirements, it is not acceptable for accelerator application.

At GSI this source has been optimized for accelerator operation, especially to feed the synchrotron. Consequently, the source is operated in a pulsed mode with a repetition rate up to 5 Hz, and a pulse length of up to 1 ms. Up to 15 emA of $^{238}\text{U}^{4+}$ can be provided at the entrance of the RFQ. The total extracted ion current from the ion source under these conditions is in the order of 150 mA.

Several measures were applied to Mevva sources to influence the source behaviour:

- | | |
|--|---|
| – discharge current | plasma density, charge state distribution, noise. |
| – magnetic fields to control discharge impedance | charge state distribution. |
| – additional gas feed | charge state distribution. |
| – geometry | charge state distribution. |

Because of the explosive character it is not surprising, that the ions as well as the electrons do have a velocity component which is not neglectable. Depending on discharge current and strength of the magnetic field up to 160 eV have been measured for the ions, respectively up to 30 eV for the electrons.

This has influence on the thickness and location of the plasma boundary.

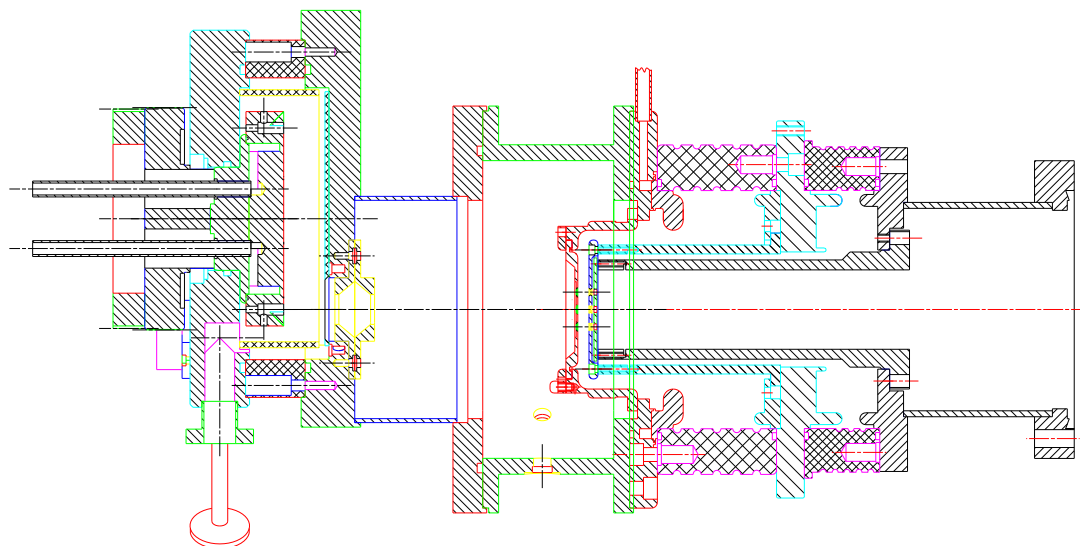


Fig. 15: Mevva ion source

Further reading: I.G. Brown in Ref. [7].

3.2.9 Laser Ion Sources (LIS)

Similar to the vacuum arc ion sources, the required element is provided as target material, which is irradiated by focused laser light of very high power density. The small surface spot will be explosively ablated and ionized. The charge state distribution is frozen shortly after leaving the surface. Although the length of the laser pulse is in the order of ns, longer pulses are available by simply letting the plasma drift for a certain length before extraction. Because of a high momentum spread, the plasma 'debunches' to a longer pulse length. To get an ion beam with constant energy along the pulse will require a slightly ramped extraction voltage.

Up to now, reliability of pulse-to-pulse reproducibility is the strongest concern of this source type. The state of the target surface is a critical issue. This is understandable because the laser power density changes drastically as soon as the surface is eroded away. The usage of liquid metallic surfaces could overcome that problem, at least for elements available in that state.

Whereas the starting energy of ions have been measured with up to several keV, the energy of electrons have not been measured yet. This makes the exact determination of the extraction impossible.

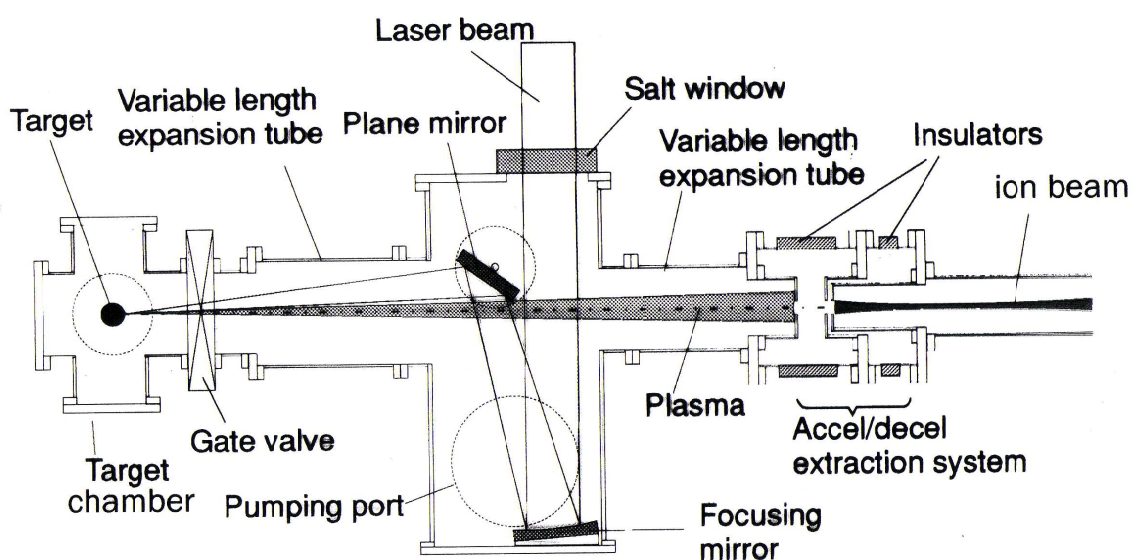


Fig. 16: Laser ion source

Further reading: B. Sharkov in Ref. [8].

3.2.10 Liquid Metal Ion Sources (LMIS)

This source type is known for its small emittance. A film of liquid metal covers a sharp needle and by applying a high electrostatic field ions are created at the surface of the needle.

Further reading: L.W. Swanson in Ref. [7].

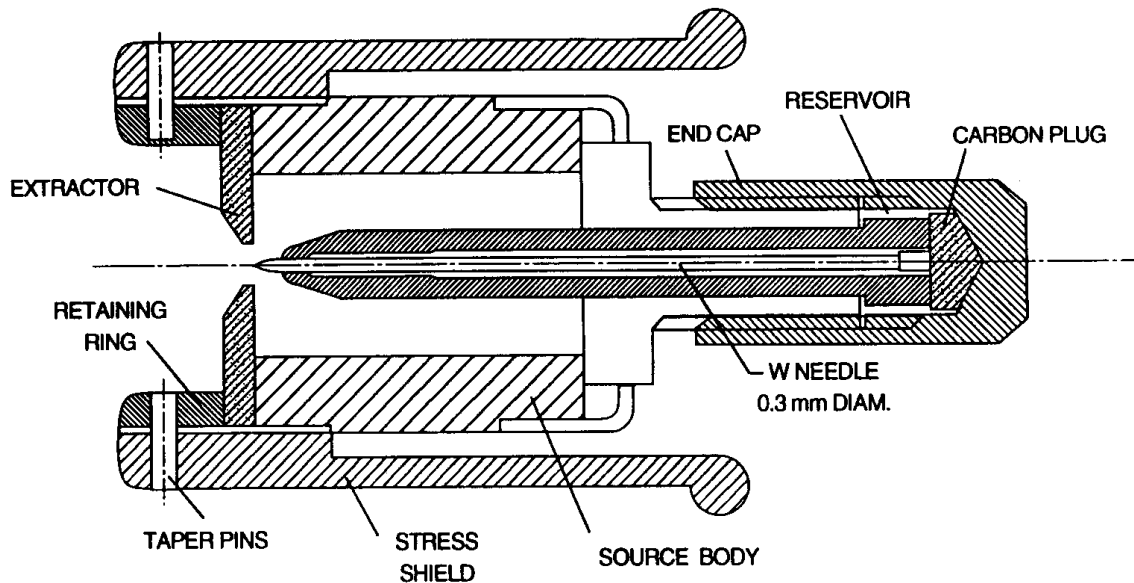


Fig. 17: Liquid metal ion source

3.2.11 Electron Beam Ion Sources (EBIS)

Electron beam ion sources provide the highest possible charge states up to bare nuclei. Compared to the 'simple' theoretical background, the technological problems are severe.

In this source the ions are stepwise ionized by an electron beam. The ions are trapped inside the source during the ionization process and extracted afterwards. The electron beam energy has to have at least the energy necessary to remove the requested electron from its shell, see Fig. 5. This means in the order of 100 keV or above for bare uranium ions.

Because of the small cross-section for ionization the electron density j_e must be high. To achieve highest possible current densities the electron beam is compressed by entering a strong magnetic solenoid, created by a superconducting coil.

To reduce recombination losses inside the source, the residual gas pressure should be less than 10^{-12} mbar.

To achieve high confinement times up to seconds, the ions are to be trapped for that time. In radial direction, this trap is provided by the space charge potential of the electron beam modified by a number of surrounding drift tube electrodes to modify the trap in longitudinal direction.

Changing the potential of the drift tube close to the extraction will open the trap for extraction.

Further reading: E.D. Donets in Ref. [7].

3.2.12 Negative ion sources

For some applications negative ions are required. The physics of the ion generator has to be changed totally, whereas for positive ion sources the ionization process is most important, electron attachment is of importance. On the other hand, one should not be surprised, to get negative ions from any ion source by simply reversing the polarity of the extraction voltage. However, an important measure will be the number of negative ions as well as the ratio of negative ions and electrons in the extracted beam.

For the plasma generator at least two different types are in use:

- surface ionization sources
- volume production sources

To increase the number of negative ions a transverse magnetic filter can be applied. This is to separate hot electrons in the discharge region from cold electrons in the extraction region. These cold electrons are required for the attachment process.

In a second step it might be useful to separate electrons from negative ions so as not to load the extraction power supply and to remove the electron beam at the lowest possible power dissipation. This can be done by a two-step extraction in accel–accel mode with an imposed transverse magnetic field. Such a combination allows the electron beam to be dumped behind the first acceleration gap. But the negative ions will be bent also. This can be corrected by appropriate steering, for example by electrode displacement, or a tilt angle between the electrodes in the second gap.

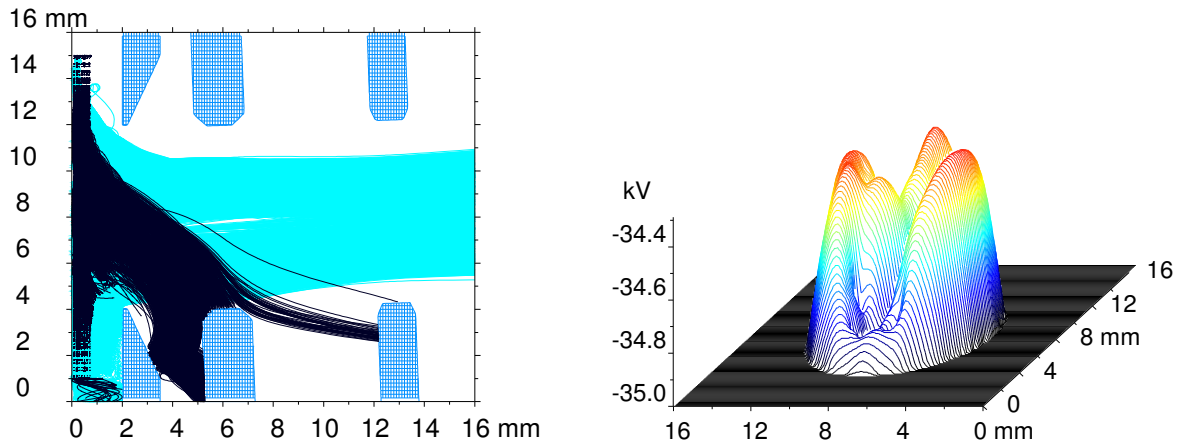


Fig. 18: Beam envelope of the extracted ion beam under the influence of the magnetic filter field and tilted electrodes. Most electrons are trapped within the plasma, or dumped on the electrode (left). However, if the plasma boundary is not perfectly matched, some electrons can be extracted. Potential perpendicular to the beam direction in front of the plasma electrode. The electrons bent out from the ion beam cause a nonlinear force (right). Simulation made with KOBRA3-INP [11].

In the example shown, a plasma potential of 0 V with respect to the plasma electrode is assumed. The positive and negative ions are assumed to have a temperature of 1 eV. 75 mA H^- are extracted with 5 kV applied to the first gap, and 30 kV voltage drop in the second gap. The output emittance is shown in Fig. 19. The space charge of the electrons is not symmetric, therefore a nonlinear force will influence the H^- -beam, see Figs. 18 and 19.

Further reading: K.N. Leung in Ref. [7].

4 Extraction

The geometry of extraction is important. Either circular holes or slits can be used. Which geometry is to be preferred might depend on the application.

The interface between the individual plasma and the extracted ion beam is another important region where the beam quality is determined. Only a few theories describing this region are available, the best known model has been developed by Self [5]. This one-dimensional model describes the electron density n_e for positive ion sources as function of the potential difference Φ to the plasma potential Φ_p and the electron temperature kT_e in fraction of the electron density in the undisturbed plasma n_{e0} .

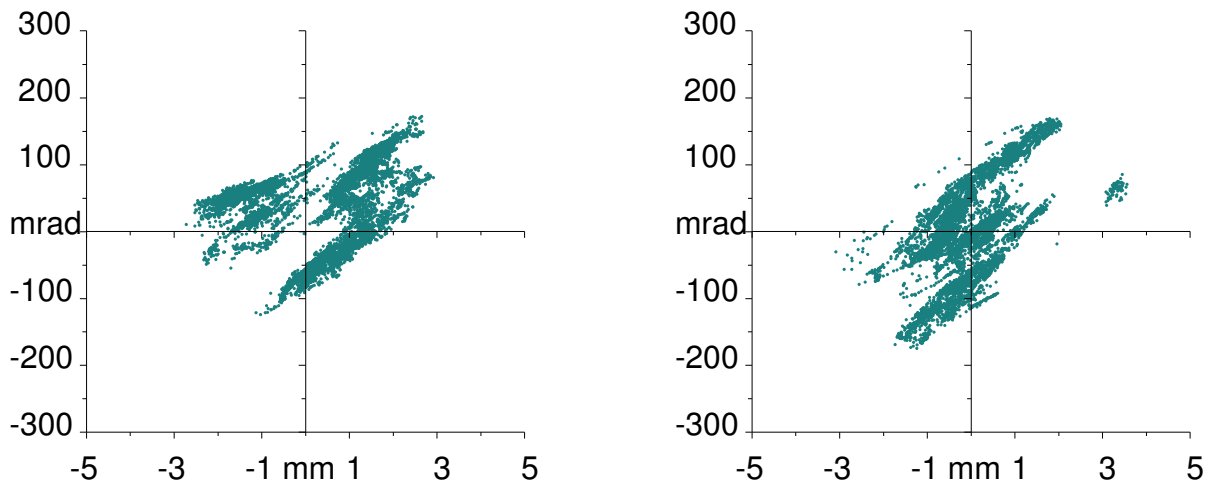


Fig. 19: Both transverse emittances of the extracted ion beam, left $\parallel \vec{B}$, right $\perp \vec{B}$

$$n_e = n_{e0} \cdot e^{-\frac{\Phi - \Phi_p}{kT_e}}. \quad (14)$$

With increasing plasma pressure the location of this plasma boundary will move towards the extraction aperture, see Fig. 20.

The hole diameter should have a certain relation to the extraction gap width, which is called the aspect ratio. Any shaping, especially at the electrode where the ions still have low energy might be useful to influence the shape of the beam. If the gap width has been fixed a maximum extraction voltage can be estimated. If the extracted beam current is not sufficient, a multi-aperture extraction system can be used, on the cost of a larger emittance, see Fig. 21.

Sometimes curved extraction systems are in use to enforce certain beam properties:

- concave electrodes to enforce a focused beam, even that the single beamlets might be divergent.
- convex electrodes to enforce a broad beam.

A similar effect can be achieved by electrode displacement. This indicates on the other hand, that the extraction holes have to be perfectly aligned to avoid beam steering.

5 Drift

Depending on current and velocity the space charge will cause severe limits of beam transport. But, as usual Mother Nature can help: the drifting ions collide with residual gas atoms. Depending on the collision, this residual gas atom can be ionized. The electron is trapped within the space charge potential of the extracted beam. The positive residual gas ion will be repelled out of the beam.

Other ions might hit the extraction electrodes, the beam tube, or other metallic surfaces (Faraday cups, slits, grids, etc.). All these secondary electrons will contribute to the compensation of space charge. With that, the space charge potential will be lowered, as long as the remaining temperature of the compensating electrons is low enough to be captured. Otherwise only cold electrons will be trapped, higher energy electrons escape. Therefore the electron temperature of these electrons within the beam gives an upper limit of space charge compensation.

This concept can work only, if no leakage of electrons makes the loss rate of electrons larger than the creation rate of electrons. One leakage for electrons is the ion source with its positive potential. On

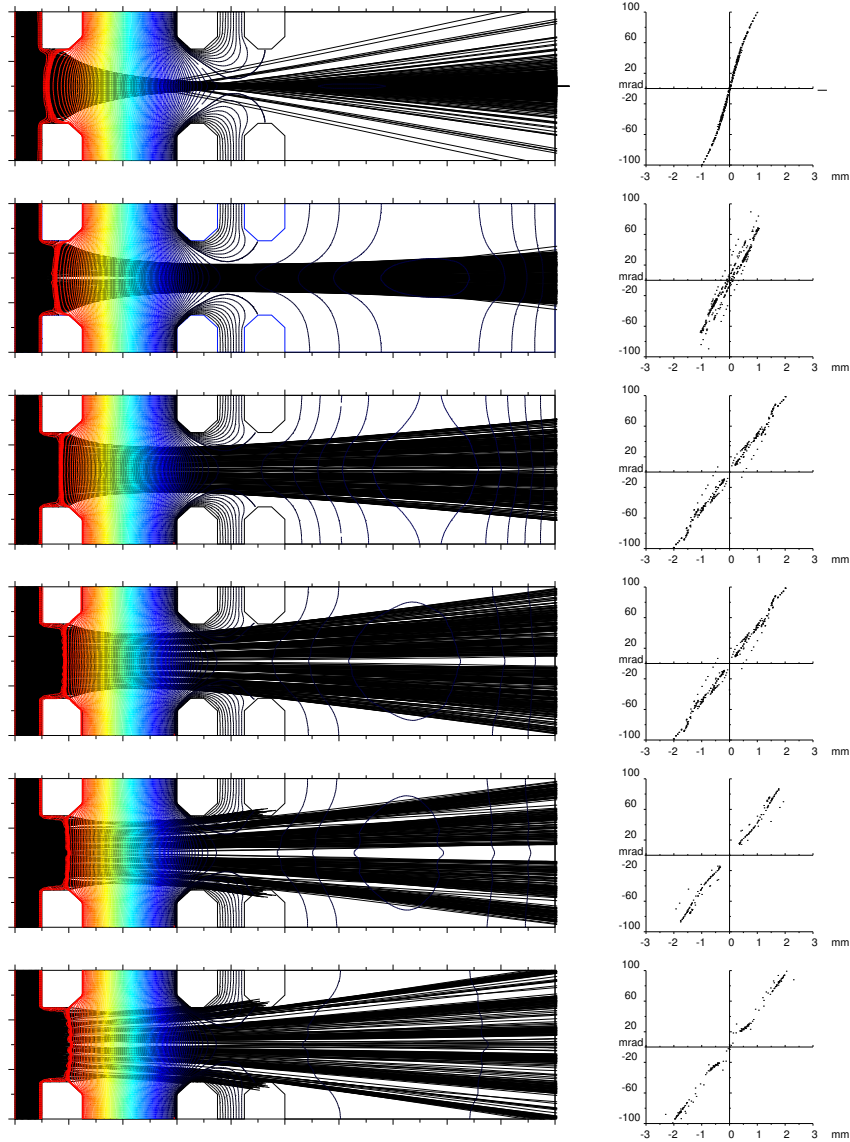


Fig. 20: Computer simulation of the extraction with an accel-decel system. The current density within the plasma has been changed from 50 mA/cm^2 (top) in steps of 50 mA/cm^2 to 300 mA/cm^2 (bottom). The plasma boundary is indicated by plotting a few potential lines between plasma potential and the potential of the plasma electrode.

one side the ions become extracted, on the other hand, electrons will be extracted from the beam towards the ion source. This can be avoided with a three electrode system, working in accel-decel mode (see Fig. 22).

For the decision on how the beam transport is to be planned, the question of space charge compensation arises. In case of an uncompensated transport the beam will double its diameter r_0 after a drift of L according:

$$L \propto r_0^4 \sqrt{q/m} / \sqrt{P} \quad (15)$$

where P denotes the perveance of the beam. A few examples given in Table 1 favour a space-charge-compensated transport.

In the simulation the difference between space charge compensated and uncompensated transport

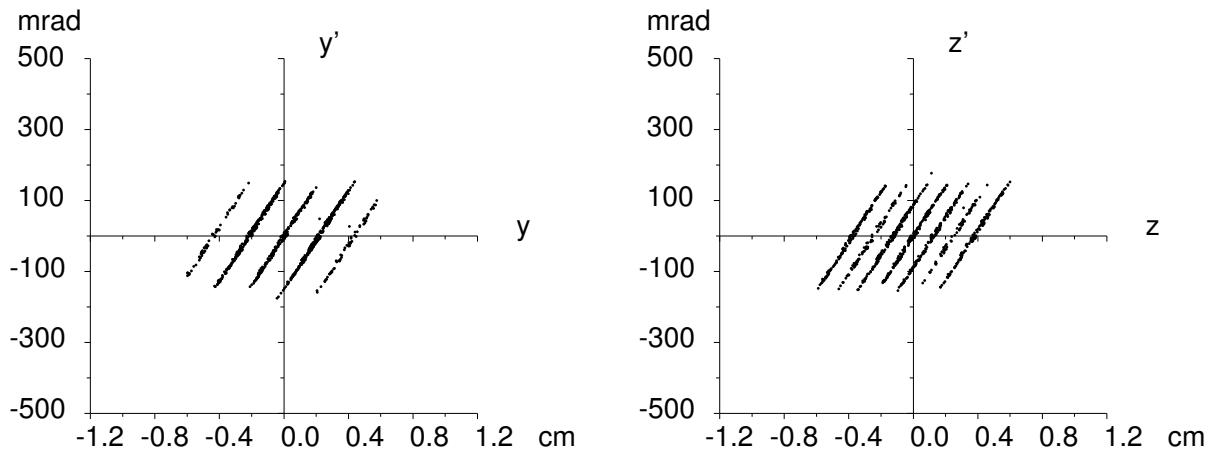


Fig. 21: Emittance of a beam extracted by a multi aperture extraction system with 13 holes

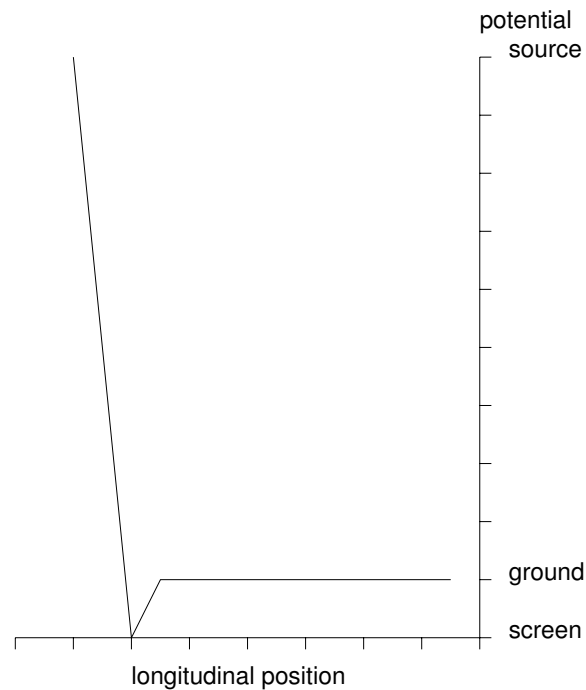


Fig. 22: The negatively biased 2nd electrode has to produce a negative potential dip on axis of the extraction hole. This screens the electrons from acceleration towards the positive potential of the ion source.

is shown in Fig. 23, where both beam emittances 230 mm behind the plasma electrode are compared. The maximum divergence angle of the r.m.s. emittance, caused by a 3 mA He beam with 12.5 keV, increases from 100 mrad to 140 mrad already after 20 cm drift.

6 Influence of space charge compensation

As already mentioned, the beam is space charge compensated under certain experimental conditions. If the loss rate becomes comparable to the generation rate a partial space charge compensation may occur. The effect will be demonstrated in the following example: Within a beam tube with length of 1 m and 80 mm diameter a singly charged Argon ion beam with 10 emA current and 30 keV energy is drifting. The absolute starting emittance is 100 mm mrad. In Fig. 24 the beam envelope is shown for the case of

Table 1: Characteristic length L for doubling the initial beam radius r_0 under the influence of space charge. The numbers are given for 1 mA electrical current and 10 mm initial beam diameter. U_{ex} is the extraction voltage, Φ_b the potential drop across the beam.

	$U_{\text{ex}}[\text{V}]$	$\Phi_b[\text{V}]$	$L[\text{cm}]$
e	-15000	-0.715	430
p	15000	30	40
Ar ⁺	15000	189	16
Ar ³⁺	5000	189	9
Ar ³⁺	15000	109	20

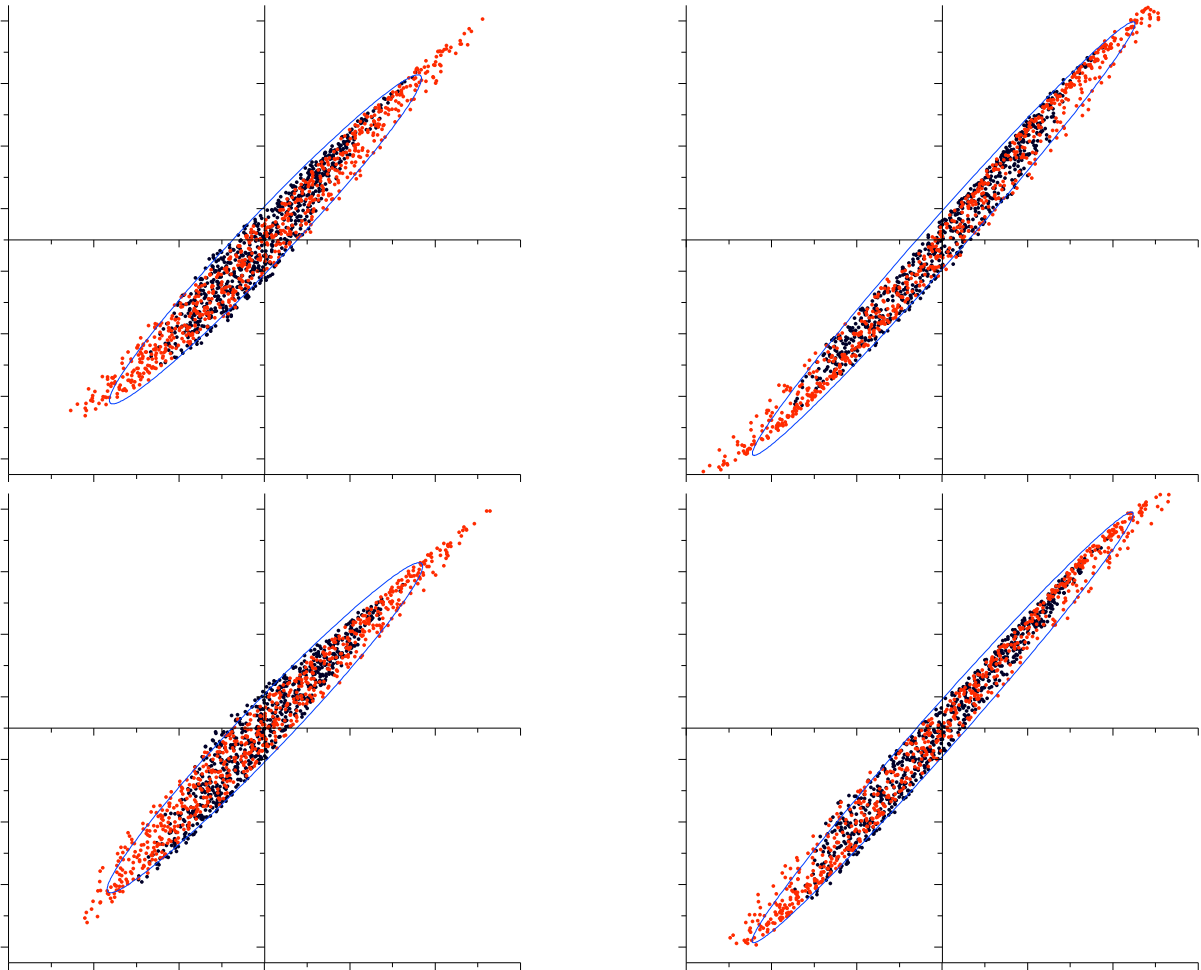


Fig. 23: Influence of compensation behind the screening electrode on the beam divergence. Scaling is ± 150 mrad and ± 30 mm; left: compensated beam, right: uncompensated beam (3 mA at 12.5 keV). Top: vertical, bottom: horizontal.

zero current (a) and for the 10 emA case (b). The compensation of an ion beam can be described using Self's [5] model similar to the physics which describes the particle distribution at the plasma boundary of an ion source in the extraction system. Using this model a much more realistic description of the ion beam transport is obtained compared to the assumption of a net current, both shown in Figs. 24 and 25. The resulting potential due to the space charge for the uncompensated beam is in the order of 800 V [Fig. 25 (a)] and the beam becomes strongly divergent [Fig. 24 (b)]; the potential drops in the longitudinal direction because of this divergence. Using a net current model, the potential is only 80 V, according to

the degree of space charge compensation [Fig. 25 (b)] and the longitudinal drop is lower because the divergence is smaller. Using Self's model the beam plasma potential is constant in the beam direction [Fig. 25 (c)] and a gradient is present at the beam edges only; the strength of the gradient depends on the electron temperature. The electrons are oscillating in the beam potential and only the coldest electrons will stay within the beam.

The effect of these different assumptions becomes clearer by observing the emittance at the end of the drift section (see Fig. 26): a pure drift without any space charge results in the emittance shown in Fig. 26 (a), strong losses and a divergent beam for the full space charge of 10 emA in Fig. 26 (b), a divergent beam but still with an undisturbed emittance for the homogeneous 1 emA beam in Fig. 26 (c), and aberrations caused by the nonlinear field of a partially uncompensated beam in Fig. 26 (d). A beam halo develops because of the gradient of the space charge potential at the beam edge. The degree of space charge compensation in Fig. 26 (c) and in Fig. 26 (d) is similar at about 90%. In Fig. 25 the potential

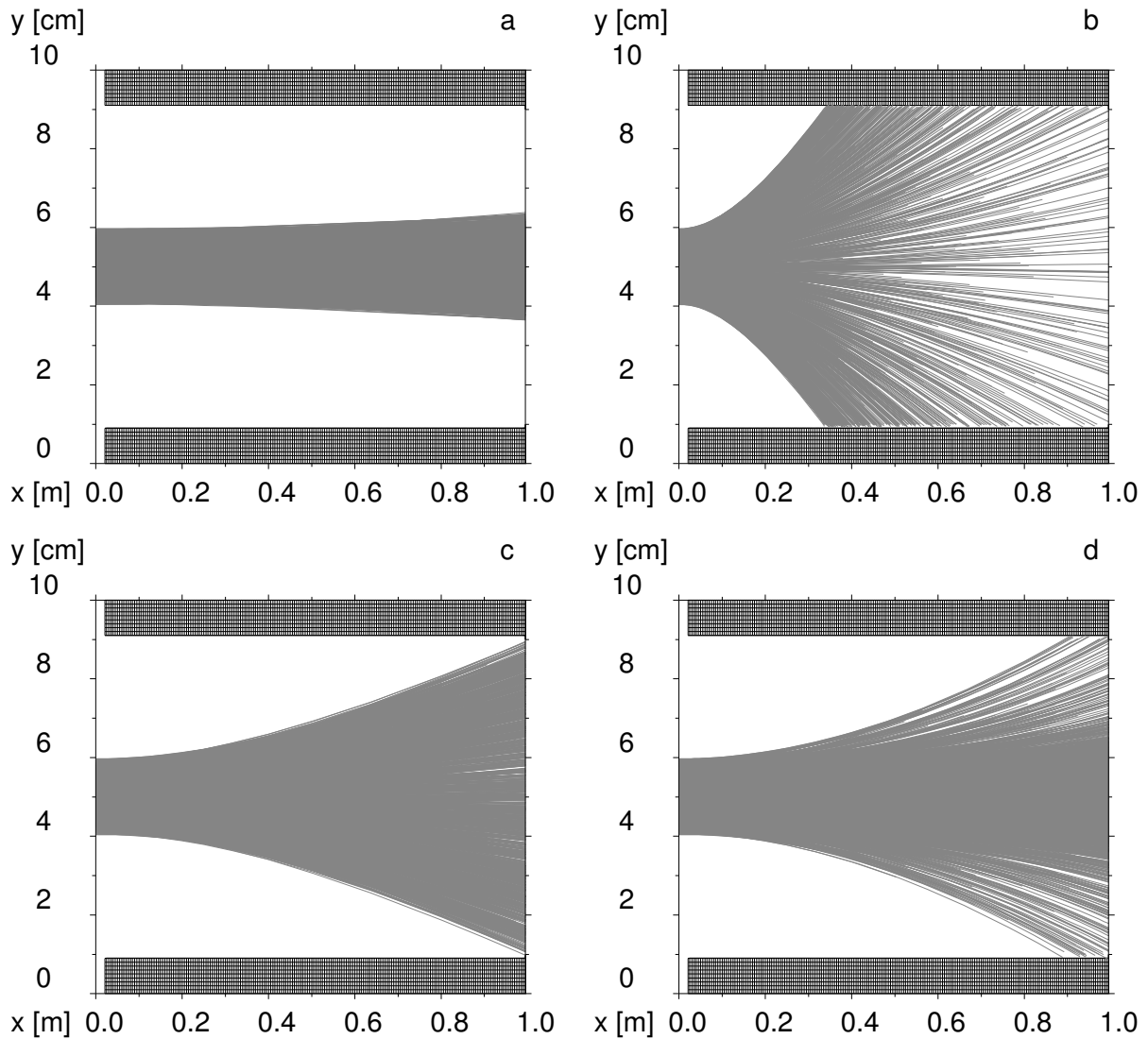


Fig. 24: Beam envelope for a drifting beam: a) no space charge, b) full space charge, c) net current, and d) space charge compensation with the beam plasma model

caused by the effective space charge is shown. The potential is plotted on the vertical axis against the

longitudinal and one transverse axis. Because of trapped electrons the potential is constant with beam plasma potential 25 (c). The gradient in longitudinal direction for 25 (b) is less strong because the beam does not diverge as strongly as in 25 (a).

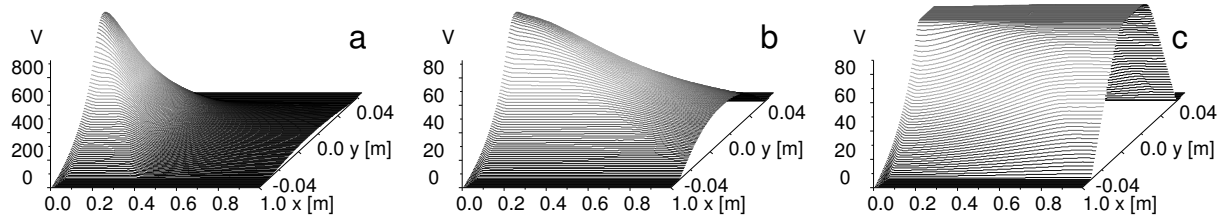


Fig. 25: Space charge potential for a drifting beam: a) full space charge, b) net current, and c) space charge compensation with the beam plasma model

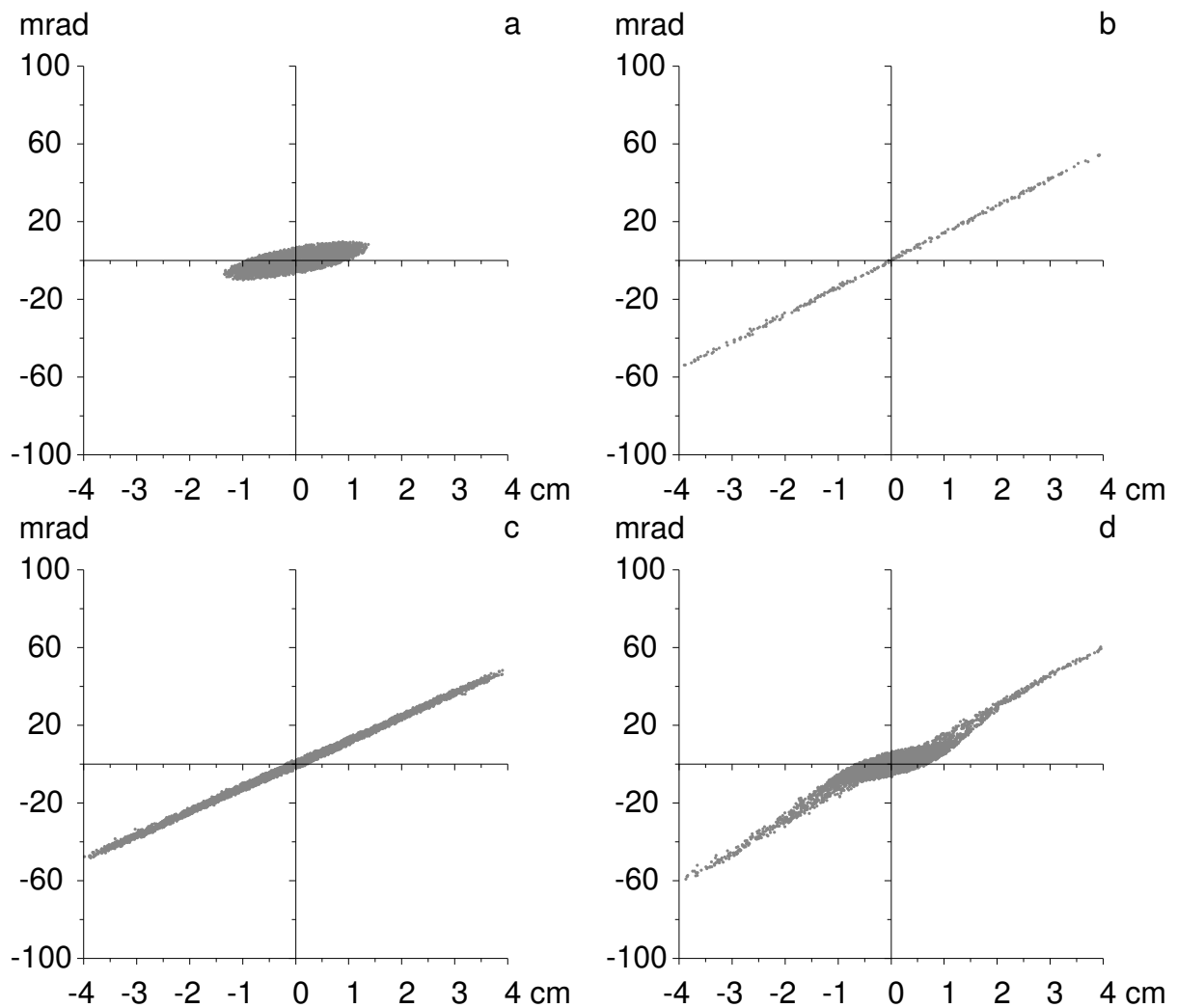


Fig. 26: Beam emittance for a drifting beam: no space charge a), full space charge b), net current c), and space charge compensation with the beam plasma model d)

The conclusions of this simulation are

- provide a very high degree of space charge compensation within the beam transport system, to keep nonlinearities small.

- remove the space charge neutralization totally, which might be even more complicated than to keep it, and provide lenses with enough focusing power.
- make the beam transport system as short as possible to reduce emittance growth along the beam line due to the imperfect neutralization.

7 Post Acceleration

A drift tube linac or a RFQ require a precise input velocity of the ions, to be in phase with the accelerating rf. If the extraction voltage is too low (too high) to achieve this velocity a dc post acceleration gap (deceleration gap) has to follow the extraction system. However, one should keep in mind that the optic of such a gap depends on field strength, and that an existing space charge compensation will be removed from the beam when entering the acceleration gap. A beam plasma boundary will develop. Again, the thickness of this plasma boundary depends on the electron temperature. Behind that sheath an eventually non homogeneous ion distribution tends to rearrange itself to become homogeneous on the cost of an increase of emittance [6].

It should be pointed out that such an acceleration gap, respectively deceleration gap should be designed as triode working in accel-decel mode, to screen eventually existing space charge compensation from the acceleration field.

Further reading: Ref. [9]

References

- [1] J.R. Pierce, Theory and Design of Electron Beams (Van Nostrand, Toronto, 1954).
- [2] P.W. Haskes, and E. Kasper, Principles of Electron Optics I, II (Academic Press Inc, 1989).
- [3] C.D. Child, Phys Rev. (Ser. 1) **32** (1911) 492.
- [4] I. Langmuir and K.T. Compton, Rev. Mod. Phys. **3** (1931) 251.
- [5] S.A. Self, Phys. Fluids **6** (1963) 1762.
- [6] Handbook of Ion Sources, edited by B. Wolf (CRC Press, Inc., 1995).
- [7] The Physics and Technology of Ion Sources, edited by I.G. Brown (John Wiley & Sons, New York, 1989).
- [8] The Physics and Technology of Ion Sources, edited by I.G. Brown second, revised and extended edition (Wiley-VCH, Weinheim, 2004).
- [9] Emerging Applications of Vacuum-Arc-Produced Plasma, Ion and Electron Beams, edited by E. Oks and I.G. Brown, Nato Science Series (Kluwer Academic Publishers, 2002).
- [10] Electron Cyclotron Resonance Ion Sources, 16th International Workshop on ECR Ion Sources, edited by M. Leitner, AIP Conference Proceedings, Vol. 749 (AIP, Melville, New York 2005).
- [11] KOBRA3-INP, INP, Junkernstr. 99, 65205 Wiesbaden, Germany.
- [12] Electron Cyclotron Resonance Ion Sources and ECR Plasmas, R. Geller (IOP Publishing Ltd., 1996).
- [13] Untersuchung einer Elektron-Zyklotron-Resonanz-Ionenquelle mit gepulster magnetischer Extraktion, C. Mühle, Dissertation, University Frankfurt, 1995.